In Situ Short-Term and Long-Term Rockfill Compressibility as a Function of Void Ratio and Strength of Parent Rock

Mohammad Kermani[1]; Jean-Marie Konrad[2]; and Marc Smith[3]

Abstract: This article presents a study on 15 concrete face rockfill dams (CFRDs) carried out to characterize in situ rockfill compressibility. The stress-strain-time behavior of rockfill for each CFRD was evaluated at the embankment centerline, during and after construction and before the onset of reservoir impoundment. By comparing the behavior in different case studies, the rockfill in situ compressibility parameters were defined and related to key material properties. It was shown that short-term and long-term response of rockfill to changes in stress level is a function of two parameters: the strength of individual rock particles and the void ratio of the rockfill assemblage. Moreover, the time-dependent and short-term rockfill compressibility parameters are connected. This study provides a good framework to characterize and estimate the behavior of rockfill during and after construction of embankments. Moreover, the concepts presented in this paper can be used for predicting postconstruction deformations of structures constructed by using compacted rockfill on the basis of their behavior during construction. **DOI: 10.1061/(ASCE)GT.1943-5606.0001835.**

Author keywords: Concrete face rockfill dams (CFRDs); Rockfill; In situ; Compressibility; Time dependent.

Introduction

Rockfill is defined by large grains (an average size of at least 5 cm and a maximum size of up to 2 m), and its variety of particle sizes, shapes, and minerals. As a consequence, an experimental study on a given rockfill material as in the field is almost impossible in the laboratory. Scale effects are shown to affect the representativeness of the laboratory results significantly (Marsal 1967; Marachi et al. 1969). Although much effort has been made to model the effect of particle sizes on mechanical behavior of rockfill (e.g., Tavares and das Neves 2008; Alonso et al. 2012, 2013), its effect is still not fully quantifiable. Additionally, the field stress paths cannot be perfectly reproduced in the laboratory. This makes the use of laboratory testing to determine the actual mechanical properties of rockfill difficult. The most reliable means to study this matter is still through well-instrumented rockfill structures. Therefore, in this study, a database of 15 concrete face rockfill dams (CFRDs) was used to investigate the in situ mechanical behavior (short-term and time-dependent compression) of the rockfill used in their construction.

Definition of Compression

In geotechnical engineering, one-dimensional compression (compressibility, when referring to the material property) is typically the uniaxial loading of an earth material in oedometric conditions, i.e., when lateral deformations are fully constrained or are assumed to be negligible. Time-dependent (or secondary) compression (time-dependent compressibility, when referring to the material property) refers to the periods when the axial load is kept constant and the material continues to deform with time.

Usually, CFRDs can be assumed to have a symmetrical geometry and to be constructed of similar materials throughout, unlike other types of rockfill dams. Therefore, they can be considered as homogeneous embankments with negligible lateral deformation at the centerline (especially in the lower levels of embankment). Consequently, before the onset of impoundment, the boundary conditions of rockfill zones at the CFRD centerline can be assumed to be close to that in an oedometer test. Different fill placement phases can be associated with different loading stages during laboratory oedometer testing. Thus, in this study, to characterize the short-term rockfill compressibility, the in situ stress-strain behavior of a rockfill layer near the centerline of the embankments during construction was considered. Similarly, the postconstruction period before the onset of impoundment was associated with the secondary compression phases in laboratory oedometer testing (to characterize time-dependent rockfill compressibility). Based on these evaluations, the dominant parameters that influence short-term and time-dependent rockfill compressibility were identified.

Background

Evaluation of and comparison between the deformation behavior of diverse rockfill dams have been the subject of numerous studies (Sowers et al. 1965; Clements 1984; Dascal 1987; Pinto and Marques Filho 1998; Hunter and Fell 2003; Milligan and Coyne 2005; Won and Kim 2008). These studies imply that several parameters influence the in situ rockfill short-term and long-term deformation behavior. The most important factors include rock particle mineralogy and strength, degree of compaction, particle shape and gradation, embankment geometry (especially dam height and valley shape), and rock particle susceptibility to strength loss caused by wetting. However, excluding Hunter and Fell (2003), the effect of influencing parameters has not been quantified on a consistent basis in these studies.

[1]Geotechnical Engineering Analyst, GHD, 4600 Blvd. de la Côte-Vertu, Montreal, QC, Canada H4S 1C7 (corresponding author). E-mail: kermani.mhmmd@gmail.com

[2]Professor, Dept. of Civil and Water Engineering, Laval Univ., 1065, Ave. de la Médecine, Pavillon Adrien-Pouliot, Room 2912B, Québec, QC, Canada G1V 0A6.

[3]Geotechnical Engineer, Dam Safety Division, Hydro-Québec, 75, Blvd. René-Lévesque Ouest, Montréal, QC, Canada H2Z 1A4.

Note. This manuscript was submitted on December 7, 2016; approved on August 16, 2017; published online on January 17, 2018. Discussion period open until June 17, 2018; separate discussions must be submitted for individual papers. This paper is part of the ***Journal of Geotechnical and Geoenvironmental Engineering***, © ASCE, ISSN 1090-0241.

Hunter and Fell (2003) studied the stress-strain behavior of rockfill in several CFRDs and concluded that the rockfill compressibility is a function of D80 size (size from which 80% of the particles are finer) and unconfined compressive strength (UCS) of the intact rock. They used rockfill secant modulus (vertical estimated stress over measured strain) at end of construction as the indicator of rockfill compressibility. Hunter and Fell (2003) did not directly quantify the effect of compaction effort and gradation while establishing a relationship between the rockfill properties and compressibility. As for the time-dependent deformation behavior, they studied the rate of crest settlement relative to dam height. They measured the average rate for each studied CFRD during the years after impoundment and commented that this rate is a function of dam height, compaction method, and UCS of intact rock.

Contrary to the work by Hunter and Fell (2003), in this study, the vertical stress-strain characteristics for a rockfill layer in the CFRD cases were studied including stress levels corresponding to different construction stages, and not only the end of construction. Because the rockfill compressibility is stress-level dependent, consideration of the whole dam construction period, and consequently, characterizing rockfill compressibility at different stress levels allowed better insight into the rockfill mechanical behavior. The average measured void ratio of rockfill at placement was also considered to mirror both the degree of compaction and rock particle-size distribution. Although the relative density is a more descriptive parameter, void ratio was used because the necessary data were not available for the studied CFRDs. Moreover, the rockfill post-construction compression behavior was studied only before the onset of reservoir impoundment, when stress distribution within the rockfill embankments is easily calculable. This allowed a better characterization of the in situ time-dependent mechanical behavior of rockfill. In addition, for each CFRD the short-term rockfill compressibility was compared with long-term compressibility, which allowed the development of a relationship between rockfill behavior during (loading stage) and after construction (constant load stage).

Although CFRD cases were used because of the simplicity of their structure and loading conditions, the results of this study can be used to characterize the behavior of rockfill materials in other rockfill dam types, railway-or-highway embankments, and other rockfill construction works.

Mechanism of Rockfill Deformation

It is widely accepted that, for most of the applied stress ranges in rockfill dams, the short-term and time-dependent compressibility of rockfill is highly dependent on particle breakage. Breakage is the result of crack propagation inside particles. Considering the classical theory of fracture mechanics and according to subcritical crack propagation phenomenon, Alonso (2003) elaborated that the rate of crack propagation depends on the stress intensity factor of the crack, K. The K factor is a function of applied stress, geometry of the problem, the length of crack, and the loading mode (whether it is tension or shearing normal, or parallel to the fissure).

When a load increment is applied to rockfill, particle cracks with stress intensities higher than a critical value (fracture toughness K^C) propagate immediately, particles break, and an instantaneous increment of strain takes place (associated with short-term compression). Cracks with stress intensities smaller than K^C but greater than the limit value (stress corrosion limit, K^0) propagate with time until failure and cause rockfill time-dependent deformations. Using theoretical thermodynamics introduces a direct relationship between velocity of crack propagation, stress intensity factor, and relative humidity of the air in connection with crack tips. Relative humidity also influences the K^0 value (Alonso 2003).

Studied Cases

The CFRDs chosen for this study were cases with detailed data on internal settlements during construction, postconstruction crest settlements, and materials specifications and embankment geometry. A summary of characteristics for the studied cases is presented in Table 1. Some of the information in this table is directly used in this study. However, some data are only presented for comprehensiveness and to allow the reader to exercise further judgment. For instance, the compaction specifications of each dam are mentioned by presenting volumetric percentage of water added to rockfill, thickness of the rockfill layers, and number of passes and weight of compactors. The properties of rockfill presented in Table 1 mostly refer to rockfill used in the centerline and levels below the lower half of dams.

In this study, the influence of individual rock particle strength was taken into account by considering the average unconfined compressive strength of the intact parent rock, i.e., the peak strength of a uniaxial compression test on cylindrical rock samples. In Table 1, the cases are separated by horizontal lines according to their strength classification. This classification (from medium to extremely high strength) was done according to Australian code AS 1726-1993 (AS 1993), presented in Table 2.

Rockfill (Short-Term) Compressibility

Before proceeding with the CFRD cases, the typical behavior of coarse granular materials in oedometer tests will be discussed. The behavior of rockfill observed in the laboratory was adopted in this study to interpret the field data.

Typical One-Dimensional Compression (Oedometer) Tests on Coarse Granular Materials

In various laboratory oedometer tests on granular materials performed at typical rockfill dam vertical stress levels (usually lower than 3 MPa), the stress-strain curves included two distinct parts.

First, according to McDowell and Bolton (1998) (as elaborated by Oldecop and Alonso 2001), at vertical stresses smaller than the clastic yield stress, the deformation mechanism is the rearrangement of particles. The clastic yield stress corresponds to the stress level in which the applied load causes the onset of particle crushing. In the particle rearrangement part, the stress-strain curve has a slight upward concavity but can be considered linear.

Second, at stresses higher than the clastic yield stress, the compression mechanism is considered to be particle breakage and splitting. As observed in many published experiments, the vertical stress-strain curve is linear above the clastic yield and within the typical rockfill dam vertical stress range [Kjaernsli and Sande 1963; Nobari and Duncan 1972; Marsal 1973 (as cited by Oldecop and Alonso 2001); Clements 1981; Das Neves and Veiga Pinto 1988; Pestana and Whittle 1995; Mesri and Vardhanabhuti 2009; Konrad and Boisvert 2010].

As an example, Fig. 1 presents the results of an oedometer test from a 30-cm-diameter cell carried out on dry quartz rockfill from the Romaine 2 Dam. The slopes of stress-strain curve are termed M_i and M_b for the stresses smaller and greater than the clastic yield stress σ_y, respectively. The index i stands for initial, and the index b stands for breakage.

J. Geotech. Geoenviron. Eng., 2018, 144(4): 04018009

Table 1. Characteristics of Studied Concrete Face Rockfill Dams (Data from Hunter and Fell 2002)

Dam name	Location	Maximum dam height (m)	Crest length	U/S slope	D/S slope	Rockfill source	Intact rock strength category	Maximum particle size (mm)	Rockfill dry density (t/m^3)	Average rockfill void ratio	Compaction specifications[a]
Reece	Tasmania	122	374	1.3–1	1.4–1	Dolerite	EH to VH	1,000	2.29	0.29	5–10; 1; 4; 10
Bastyan	Tasmania	75	430	1.3–1	1.3–1	Rhyolite	VH	600	2.20	0.23	20; 1; 8; 10
Cethana	Tasmania	110	213	1.3–1	1.3–1	Quartzite	VH	900	2.07	0.27	15; 0.9; 4; 10
Murchison	Tasmania	94	200	1.3–1	1.3–1	Basalt, basaltic breccia	VH	600	2.27	0.23	20; 1; 8; 10
Foz Do Areia	Brazil	160	828	1.4–1	1.4–1	Rhyolite	H to VH	600	2.12	0.33	25; 0.8–1.6; 4; 10
Shuibuya[b]	China	233	675	1.4–1	1.4–1	N/A	VH?	N/A	2.30	0.22[c]	20; N/A; N/A; N/A
Winneke	Australia	85	1,050	1.5–1	2.5–1	Siltstone	H	800	2.07	0.30	15; 0.9; 4–6; 10
Kotmale	Sri Lanka	90	560	1.4–1	1.45–1	Charnockitic/gneissic	H to VH	700	2.20	0.2[c]	30; 1.0; 4; 15
White Spur	Tasmania	43	146	1.3–1	1.3–1	Tuff	H to VH	1,000	2.30	0.21	10; 1.0; 4; 10?
Tullabardine	Tasmania	25	214	1.3–1	1.3–1	Greywacke, some slate	H	400	2.22	0.23	10; 0.9–1.0; 4; 10
Mackintosh	Tasmania	75	465	1.3–1	1.3–1	Greywacke, some slate	M to H	1,000	2.20	0.24	10; 1; 8; 10
Little Para	Australia	53	225	1.3–1	1.4–1	Dolomitic siltstone	M to H	1,000	2.15	0.22	N/A; 1; 4; 10
Scotts Peak[d]	Tasmania	43	1,067	1.7–1	1.3–1	Argillite	M	420	2.10	0.27	N/A; 0.9; 4–6; 10
Roadford[d,e]	Britain	41	430	2.25–1	2.25–1	Sandstone/mudstone	M?	400	2.07	0.32	N/A; 0.45; 8; 9.1
Martin Gonzalo[d,f]	Spain	53	N/A	1.5–1	1.5–1	Slate, greywacke	M?	700	2.15	0.26	N/A; 0.8; 6; 14

Note: D/S = downstream; EH = extremely high strength; H = high strength; M = medium strength; U/S = upstream; VH = very high strength; ? = data has been interpreted indirectly from evidences.
[a]Data have the following format: added water (% by volume); layer thickness (m); number of passes; weight of roller (t).
[b]Data from Zhou et al. (2011) and Guiyao et al. (2009).
[c]Estimated on the basis of dry density.
[d]Asphaltic concrete or membrane face rockfill dam.
[e]Data from Wilson and Evans (1991) and Evans and Wilson (1992, 1994).
[f]Data from Justo (1991), Justo et al. (1988), and Justo and Durand (2000).

Table 2. Classification of Strength of Rock according to AS 1726-1993 (Reprinted from Hunter and Fell 2002, with Permission)

Strength descriptor	UCS range (MPa)
Extremely high	>240
Very high	70–240
High	20–70
Medium	6–20

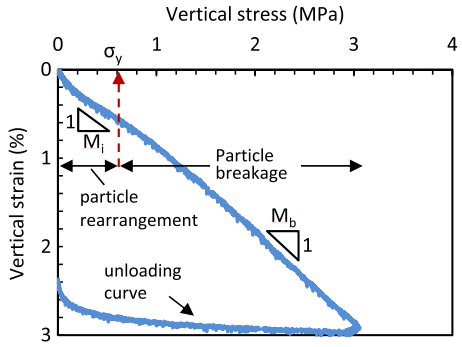

Fig. 1. Results of an oedometer test on Romaine 2 rockfill, with density of 1,830 kg/cm^3 (adapted from Konrad and Boisvert 2010, with permission)

In Situ Rockfill Compressibility

In situ rockfill compressibility was studied in a single layer at the bottom of each CFRD during embankment construction. To produce field compression curves, vertically applied stresses to rockfill can be estimated at the centerline, and the corresponding strains can be measured for each construction stage by using field-monitoring records. The method used for obtaining in situ stress and strains is explained in the following.

Determination of Field Vertical Stress-Strain Curves

Fig. 2 shows a given rockfill layer within a schematic section of a homogenous embankment for which stress-strain behavior during construction is desired. For most of the studied CFRDs, this layer was the lower third to half of the embankment height. The vertical stress value at the midheight of the given rockfill layer (representing the average vertical stress) for each construction stage was estimated from simple linear elastic solutions (Poulos and Davis 1974) with the assumption that the embankments were constructed in horizontal layers. Note that the presented vertical stress estimation method differs from that of Fitzpatrick et al. (1985), who simply estimated the vertical stress as the multiplication of fill density to fill height above the layer.

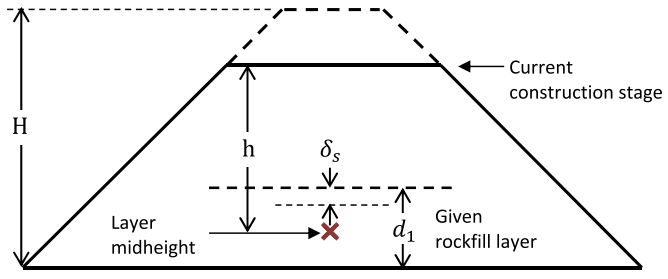

Fig. 2. Calculation of vertical stresses and strains during construction

In any construction stage, the vertical strain values were calculated by using internal settlement monitoring records for the top of the layer at the embankment centerline. Because the studied cases were constructed on rock foundations, the settlement at the bottom of the layer was considered to be negligible. Thus, for any construction stage, the strain was simply defined as δ_s/d_1, where δ_s = total vertical displacement of the settlement gauge when the current construction stage was reached; and d_1 = primary thickness of the layer (Fig. 2). Finally, the in situ stress-strain curves were drawn by using the estimated vertical stresses and calculated vertical strains.

The calculations of vertical stresses and strains are carried out for Martin Gonzalo, Foz do Areia, Roadford, and Shuibuya dams by the authors. For the other cases, the data were directly taken from Hunter and Fell (2002).

Fig. 3(a) presents the vertical stress-stain curves for the studied CFRD cases. Although the data points are slightly scattered, similar to what was observed in laboratory experiments, for most of the cases the in situ stress-strain curves can be approximated by two straight lines, as in Fig. 3(b). Here, a suffix r was added to the laboratory compression parameters to designate field values. Thus, the stress where the slope of the in situ compression curves along linear axes changes was termed σ_{ry}. Similarly, the slopes of in situ compression curves for stresses lower and higher than σ_{ry} were termed M_{ri} and M_{rb}, respectively.

In Fig. 3, the zero strain corresponds to the estimated stress at the middle of the rockfill layer, when the monitoring instrument at the top of the layer was installed. Therefore, the measured strain values in this figure are slightly smaller than in reality. The data points of each case could be slightly shifted downward to yield more realistic stress-strain curves. However, the graphs were not manipulated because using the graphs as they are does not introduce any errors neither on σ_{ry} values nor on the moduli.

The data presented in Fig. 3(a) suggest that σ_{ry} roughly falls between 0.5 and 1.0 MPa for the studied CFRDs. As observed in oedometer tests, σ_{ry} might correspond to change in compression mechanism from particle rearrangement to particle breakage. Inferring from Oldecop and Alonso (2001), Alonso (2003) and Alonso et al. (2005, 2011), the clastic yield stress is considered to vary between zero and 0.4 MPa for various rockfills according to oedometer tests. Thus, field values are significantly higher than laboratory test data. The reason might be some of the cracks on the particles grow and particles break during compaction of the studied layer in the field. Therefore, because weaker particles were already broken, higher stresses were needed for the onset of particle breakage as the construction of upper layers proceeded. Additionally, the densities in the field are usually higher than in the laboratory. For instance, in the oedometer test presented in Fig. 1, whereas laboratory samples had a dry density of 1,830 kg/m^3, the field dry densities were around 2,200 kg/m^3. Moreover, the rockfill lateral confinement is not perfect in the centerline of CFRDs; thus, there is more chance for the particles to slide and displace instead of breaking.

The necessary tensile stress (McDowell and Bolton 1998; Alonso et al. 2013) and the necessary energy (Tavares and das Neves 2008) for particle breakage decreases with increasing particle size. Particle sizes are normally larger in the field than in the laboratory. Therefore, the onset of particle breakage is expected to occur at lower stress levels in the field than in the laboratory. However, the effects of compaction prestressing, high densities, and inadequacy of lateral confinement seem to be dominant when compared with the size effect in σ_{ry}, when reviewing values obtained from the case studies.

A second hypothesis is that σ_{ry}, the stress level at which the modulus changes, can be associated with the maximum stress that

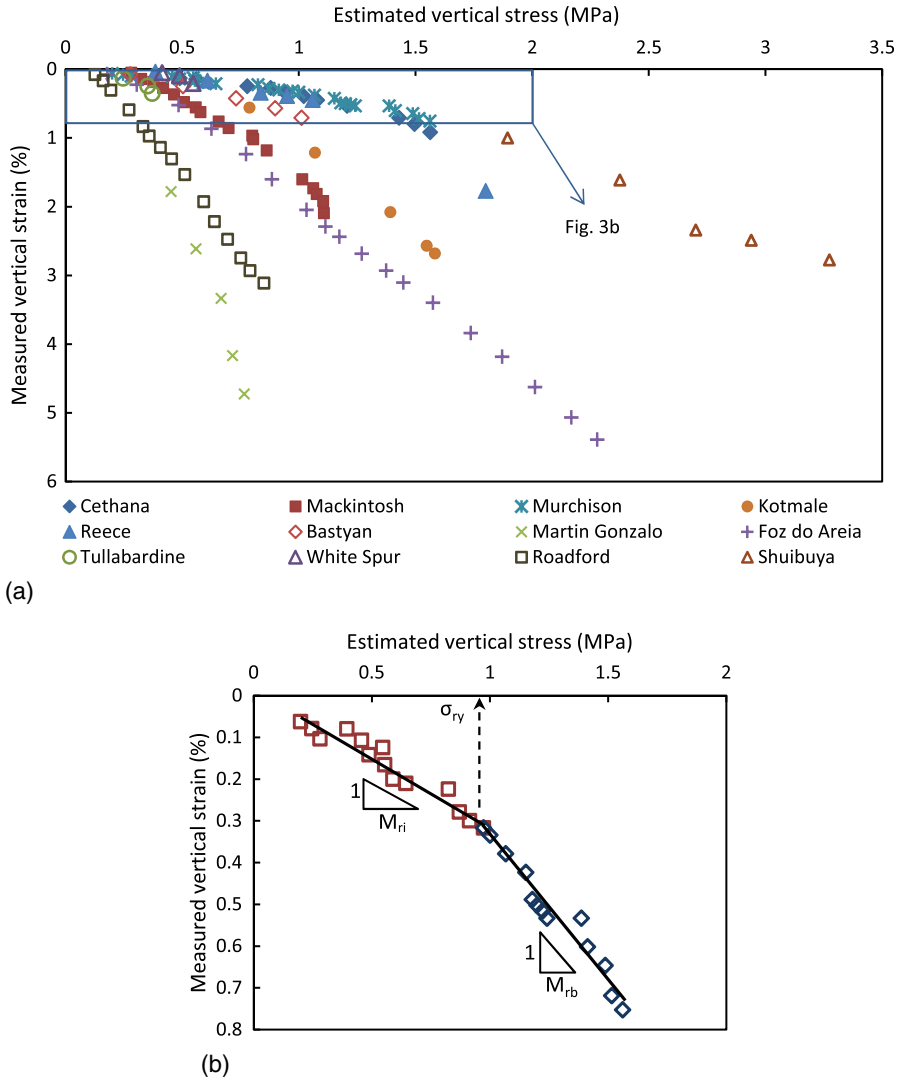

Fig. 3. In situ stress-strain relationship: (a) for rockfill of studied CFRDs (data from Hunter and Fell 2002); (b) for rockfill of Murchison CFRD

the material has previously experienced. In other words, in the studied cases, σ_{ry} may correspond to the stress applied to rockfill during the compaction process. However, no clear relationship was observed between the compaction effort and the measured σ_{ry} values for the studied cases.

In Situ Compressibility as a Function of Rockfill Index Properties

To relate the compressibility of compacted rockfill to key material properties, σ_{ry}, M_{ri}, and M_{rb} values were determined for different case studies and related to the average rockfill void ratio and UCS of the intact parent rock. The rockfill void ratio at placement is expected to correlate with the effects of degree of compaction and rock particle-size distribution. The UCS reflects the strength of individual rock particles. For the rockfill compression characterization purposes, the intact rock strength has been simplified into two classes: very to extremely high strength and medium to high strength (Table 2).

Fig. 4 shows σ_{ry} values derived for the studied CFRDs versus rockfill void ratio for different rock strength categories. Each data point corresponds to one of the CFRD case studies. For the CFRDs that only the data on stresses smaller or greater than σ_{ry} were available, this parameter could not be calculated (Table 3). In Fig. 4, σ_{ry} is generally higher for rockfills constituted of rocks with higher intact strength. Additionally, σ_{ry} is generally smaller for rockfills placed at higher void ratios. Higher strengths of intact rock can be associated with stronger bonds between minerals and the presence of fewer cracks inside the particles. Higher void ratio can be

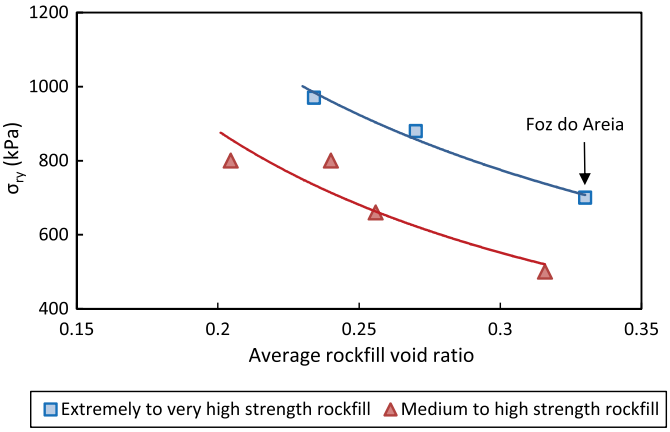

Fig. 4. Relation between in situ threshold stress, σ_{ry}, and average rockfill void ratio at placement

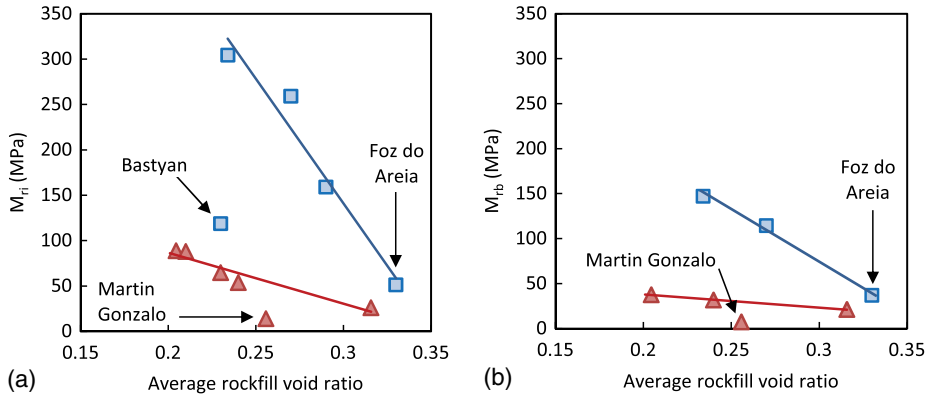

Fig. 5. Average rockfill void ratio versus (a) initial rockfill modulus and (b) rockfill modulus for stresses higher than σ_y

associated with fewer contact points between particles, and consequently, higher stresses at contact points, as well as higher stress intensity factors on the cracks within particles. Therefore, the trends observed in Fig. 4 support the hypothesis that the modulus change in the field stress strain data associates with the onset of particle breakage.

Although it is expected that σ_{ry} values increase with intact rock strength, Foz do Areia Dam has smaller σ_{ry} compared with some cases with lower intact rock strength. Fig. 4 reveals that the relatively small σ_{ry} value for rockfill in Foz do Areia Dam can be attributed to the relatively high void ratio. This reflects the importance of compaction and particles gradation even when good-quality materials are used.

Figs. 5(a and b) show the two rockfill moduli, M_{ri} and M_{rb} [as defined in Fig. 3(b)], versus average rockfill void ratio. Again, the data points are differentiated on the basis of their rock strength category. There is a clear tendency for rockfills constructed from lower-strength rock and placed at higher void ratios to have smaller moduli. This is generally true for stress levels both below [Fig. 5(a)] and above [Fig. 5(b)] the threshold stress. The reason is that for the stresses below the threshold stress, with lower strength and higher void ratio, more contact points deteriorate, which facilitates sliding of particles. Also, for the stresses greater than the threshold stress, lower strength and higher void ratio lead to higher stress intensities on the cracks inside particles causing breakage of more particles in response to the applied load increment. Consequently, throughout all stress level ranges experienced by rockfill in the studied cases, larger strains are measured for a given vertical stress with decreasing rock intact strength and increasing rockfill void ratio.

The measured moduli for Martin Gonzalo Dam's rockfill are outside the observed trend for medium- to high-strength rockfill in Figs. 5(a and b). The rockfill used in the construction of Martin Gonzalo Dam is reported to be highly susceptible to strength loss caused by wetting (Justo and Durand 2000). The abnormal compression behavior of this case is caused by settlement of the rockfill induced by excessive precipitations during construction. Additionally, the modulus obtained for Bastyan Dam lies between the data points of the two UCS categories [Fig. 5(a)]. This might be caused by the uncertainty in the intact rock UCS value for this case. The rock UCS was identified as very high, but the value was not reported by Hunter and Fell (2002). Although clear distinction was considered between the UCS categories, the UCS in this case might have been close to the marginal value between high- and very-high-strength classes, i.e., 70 MPa.

The M_{ri} value obtained for Foz do Areia Dam [Fig. 5(a)] is less than most of the cases with smaller intact rock strength. This value falls in the expected range, when considering the rockfill void ratios in Fig. 5(a). This further reveals the importance of the effect of void ratio on rockfill mechanical behavior.

In summary, in situ vertical stress-strain plot for rockfill under laterally confined conditions can be approximated with two straight lines. These lines can be characterized with three parameters: σ_{ry}, the threshold stress for the slope change, and M_{ri} and M_{rb}, which identify the slopes of the stress-strain plot at stresses smaller and greater than σ_{ry}, respectively. Figs. 4 and 5 relate these parameters to the UCS of the intact parent rock and the average rockfill void ratio at placement for compacted rockfill. These graphs can be used to calibrate a bilinear elastic constitutive model to compute the deformation of rockfill embankments during construction. When referring to these figures, rockfill with high potential for collapse caused by wetting or quarried from rocks with UCS values close to the margins of the UCS categories (defined in Table 2) must be treated with caution.

Rockfill Time-Dependent Compressibility

As explained previously, time-dependent compression refers to the deformations under constant stress in oedometric conditions. The objective in this section is to characterize the in situ rockfill time-dependent compression behavior by means of calculation from field data. To do so, the postconstruction settlement records up to the onset of CRFD impoundment were analyzed. During this period, CFRDs settle with time merely because of their self-weight. Similar to the section on short-term compressibility, before proceeding with evaluation of the data on real CFRDs, the behavior of coarse granular materials during secondary compression in the laboratory is discussed.

Typical One-Dimensional Compression Tests on Coarse Granular Materials during Secondary Compression Phase

Fig. 6 shows selected results of a one-dimensional compression test on a crushed slate with a maximum particle size of 40 mm, as indicated by Oldecop and Alonso (2007). The vertical load was applied incrementally and was kept constant for several hours in each step [Fig. 6(a)]. Fig. 6(b) shows the compression curves for strains measured at different elapsed times after load increment applications (10, 100, and 1,000 min). Typically, the slope of the compression curve (in logarithmic scale) obtained at the end of loading phases is called the compressibility index, λ. Additionally, strain versus time (in natural log scale) curves during different constant

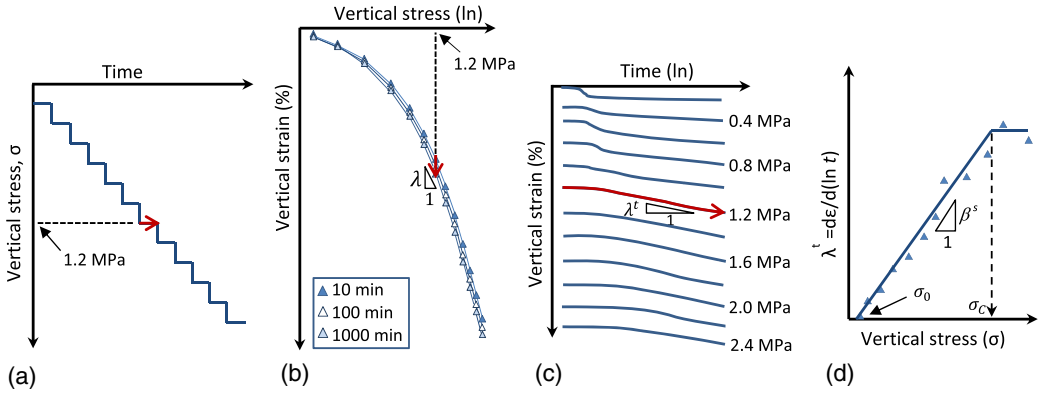

Fig. 6. Typical results of an odometer test on rockfill (crushed slate) during secondary compression: (a) loading stages; (b) compression curves; (c) strain versus time for different constant vertical loads; (d) time-dependent compression index for different stress levels; the arrows show the constant load period at 1.2-MPa vertical stress [(b, c, d) adapted from Oldecop and Alonso 2007, © ICE Publishing, with permission]

load stages are shown in Fig. 6(c). As reported by several authors (e.g., Sowers et al. 1965; Clements 1981; Parkin 1991; Oldecop and Alonso 2007; Romero et al. 2012), similar to other earth materials, during rockfill secondary compression axial strain develops almost linearly with the logarithm of time. The longest oedometer test on a rockfill sample found in the literature was carried out by Charles (1973) (as reported by Clements 1981), in which a constant vertical load of 696 kN/m^2 was applied for 3 years. The results validated the simple logarithmic relationship for secondary compression. The time-dependent compressibility index can be defined as the slope of natural logarithm of time versus axial strain curve

$$\lambda^t = \frac{d\varepsilon}{d(\ln t)} \tag{1}$$

where $d\varepsilon$ = vertical strain increment; and t = time elapsed since application of the last load increment. For instance, the time-dependent compressibility index is shown for a specific vertical stress of 1.2 MPa in Fig. 6(c).

The secondary compression is usually a function of the applied stress level. Fig. 6(d) shows λ^t values obtained at different vertical stress levels for the same test shown in Fig. 6(c). First, at stresses less than the lower limit σ_0, time-dependent deformations can practically be assumed negligible, which was also observed in oedometer or isotropic loading tests by Clements (1981), Colliat-Dangus et al. (1988), and Romero et al. (2012). Thus, σ_0 can be defined as the threshold stress for the onset of rockfill time-dependent deformations. Second, for stresses greater than the upper limit σ_c, λ^t remains almost constant. Between these two threshold stresses, λ^t is defined by a line with a slope β^s. For the oedometer tests reported by Oldecop and Alonso (2007), σ_0 and σ_c were around 200 and 2,000 kPa, respectively. The linear change in λ^t with increasing axial stress in rockfill oedometer testing is also reported by Ortega (2008) and Romero et al. (2012). Consequently, λ^t can be defined by the following expressions:

$$\text{for } \sigma \le \sigma_0 : \lambda^t \approx 0 \tag{2a}$$

$$\text{for } \sigma_0 < \sigma < \sigma_c : \lambda^t \approx \beta^s(\sigma - \sigma_0) \tag{2b}$$

$$\text{for } \sigma_c \le \sigma : \lambda^t \approx \beta^s(\sigma_c - \sigma_0) \tag{2c}$$

where all parameters are shown in Fig. 6. This feature of the rockfill compression behavior was adopted in this study to estimate the time-dependent compressibility values for different rockfill layers within an embankment with different vertical stress levels.

Assuming that, in the range of stress applied to rockfill in rockfill dams, the vertical stress is generally less than σ_c, rockfill time-dependent compression can be characterized by β^s and σ_0. By using the results raised from this assumption, it will be further validated. In this study, the in situ time-dependent compression behavior of rockfill was characterized by deriving β^s and σ_0 parameters for the rockfill used in well-instrumented CFRDs via settlement monitoring records.

In Situ Time-Dependent Compressibility of Compacted Rockfill

It was preferred to evaluate the in situ time-dependent behavior of rockfill layers through displacements of rockfill layers within the embankments with time, directly measured in the field. However, such data were not available for most of the studied cases. Instead, the time-dependent deformation behavior of rockfill layers within the embankments was evaluated by using crest settlement records with time.

Fig. 7 shows the postconstruction crest settlement relative to dam height ($\Delta H/H$) versus time elapsed since the end of construction and before impoundment for the studied CFRDs. The data points can be considered to fall on a straight line in semilogarithmic scale. Thus, relative crest settlement rate α_1 can be defined as

$$\alpha_1 = \frac{d(\frac{\Delta H}{H})}{d(\log t)} \tag{3}$$

The value of α_1 can be used as an index of the embankment postconstruction settlement. It was used in this study to infer the two parameters β^s_r and σ_{r0}. Again, the suffix r was added to the laboratory parameters β^s and σ_0 to emphasize that these parameters refer to the in situ data.

Determination of the Time-Dependent Deformations Threshold Stress, σ_{r0}

To find an estimate of the threshold stress for the onset of rockfill time-dependent deformations, the average vertical stress within the bottom rockfill layer (lower one-third of dam height) was calculated for the studied cases. Time-dependent settlements of embankments are supposed to take place mostly at this part of the dams because the stress levels are higher (see Hunter and Fell 2003 for further explanation). These stress values were then plotted versus relative crest settlement rates (α_1) of the dams, as shown in Fig. 8. It is obvious that the crest settlement rates increase with increasing

J. Geotech. Geoenviron. Eng., 2018, 144(4): 04018009

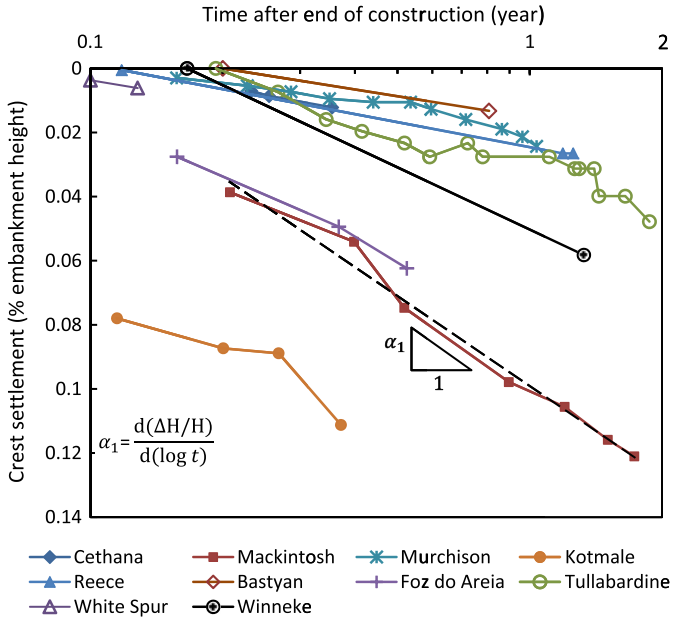

Fig. 7. Postconstruction crest settlement before the onset of impoundment for the studied CFRDs

stress levels. On the basis of the linear trend line associated with high-strength rockfills, α_1 is negligible in dams with stress less than 200 kPa at the bottom layer. Because crest settlement is the sum of settlements of internal rockfill layers, it can be implied that high-strength rockfills do not show time-dependent deformations at stresses less than 200 kPa. Thus, this stress level was assumed to be the threshold value σ_{r0} for rockfills constructed by using high-strength rocks. Similarly, α_1 would be negligible in dams constructed by using very-high-strength rockfills at stresses less than 400 kPa at the bottom layer. Thus, σ_{r0} was estimated as 400 kPa for rockfills quarried from very-high-strength rocks.

For the CFRDs with rockfill quarried from medium-strength rock, the α_1 values were well more than those of other cases (could not be shown in Fig. 8). For instance, in Martin Gonzalo and Scotts Peak, α_1 is around 0.35, whereas the stress is around 500 kPa. Moreover, for the cases with medium-strength rock, no clear relationship was observed between α_1 values and stress levels. Therefore, σ_{r0} was assumed to equal zero for rockfill constructed from medium-strength rock; i.e., time-dependent deformations take place

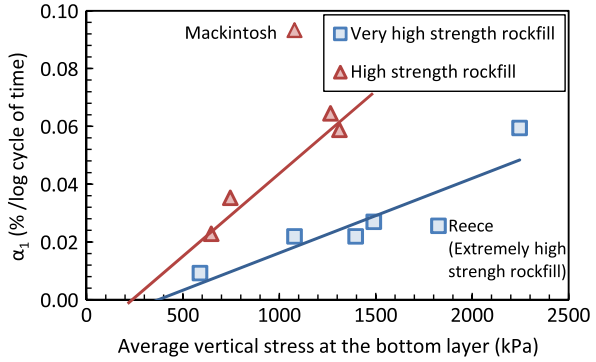

Fig. 8. Relative crest settlement rate before impoundment versus the estimated average vertical stress applied to rockfill in the lower one-third of the dam height

at any stress level. Finally, for Reece, the only case with extremely-high-strength intact rock, σ_{r0} must be greater than the value estimated for very-high-strength rockfill; hence, it was tentatively assumed to equal 700 kPa.

In Fig. 8, Mackintosh Dam was considered as an outlier because it did not follow the general observed trend. This can be attributed to factors such as embankment and valley geometry, uniform gradation of rock particles, and high construction speed. Also, no clear trend was found between rockfill void ratio and α_1 values. Therefore, σ_{r0} was assumed to be merely a function of rock UCS. The σ_{r0} values adopted for the CFRD case studies are presented in Table 3.

Determination of Time-Dependent Deformation Stress Dependency Parameter, β_r^s

To determine β_r^s values for the rockfill used in the studied CFRDs, a relationship was found between this parameter and the postconstruction crest settlement rate. At any given moment during the postconstruction period, crest settlement is the sum of settlements of different fill layers within an embankment. Therefore, the crest postconstruction settlement can be calculated as the integration of settlements of different layers along the embankment height. Fig. 9 shows a typical trapezoidal embankment. Assuming a given layer with thickness dh at a distance h from the crest, one can write

$$\Delta H = \int_0^H \varepsilon_y dh \tag{4}$$

where ε_y = vertical engineering strain of each layer at a distance h from the crest.

Considering a linear vertical strain versus logarithm of time relationship [as shown in Fig. 6(c)] for rockfill at the embankment centerline, the strain in any internal rockfill layer can be obtained

$$d\varepsilon_y = \lambda_r^t d(\ln t) \quad \text{or} \quad \varepsilon_y = \lambda_r^t \ln\left(\frac{t_2}{t_1}\right) \tag{5}$$

where t_1 and t_2 = times elapsed from the time datum (end of construction) and the beginning and the end of the desired crest settlement period, respectively. The integration constant is considered to be zero, assuming that only the strains after t_1 are considered. Suction (or the relative humidity) is assumed to be constant during the settlement period, and consequently, the λ_r^t values are assumed to change linearly with increasing vertical stress with slope β_r^s (Oldecop and Alonso 2007; Romero et al. 2012). This assumption is essential because according to Oldecop and Alonso (2007), for a given material, different β^s values were obtained for different relative humidity values in Fig. 6(d). It was also assumed that the range of stresses that apply to rockfill in dams is smaller than σ_c

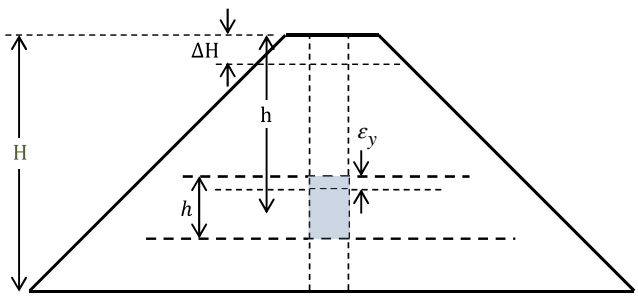

Fig. 9. Analytical calculation of crest settlement rate for a rockfill embankment

[Fig. 6(d)], to consider the changes in λ_r^t with vertical stress, Eq. (2) can be shortened to

$$\text{for } \sigma \le \sigma_{r0}: \lambda_r^t = 0 \tag{6a}$$

$$\text{for } \sigma > \sigma_{r0}: \lambda_r^t = \beta_r^s(\sigma - \sigma_{r0}) \tag{6b}$$

where σ = vertical stress in the given rockfill layer at the centerline.

Assuming a linear change in vertical stress from bottom to top of the embankment, a constant unit weight for all of the rockfill layers, and plain strain conditions in a rockfill embankment, vertical stress at any level in the centerline can be estimated as

$$\sigma \approx z\gamma h \tag{7}$$

where γ = average unit weight of above rockfill zones; and z = factor, which takes into account the effect of the embankment shape. Simple numerical modeling using linear elastic constitutive models on homogeneous trapezoidal embankments (Poulos and Davis 1974) yields parameter z values of 0.8, 0.86, and 0.88 for upstream and downstream slopes of $1.4-1$, $1.73-1$, and $2-1$ (horizontal to vertical), respectively.

According to Eq. (6), for vertical stresses lower than σ_{r0}, no time-dependent deformation takes place. Therefore, in Eq. (4) the lower limit of the integration must be set to the level where vertical stress exceeds σ_{r0}. Adopting the aforementioned considerations and entering Eqs. (5), (6*b*), and (7) in Eq. (4), the integration can be written as

$$\Delta H \approx \int_{\frac{\sigma_{r0}}{z\gamma}}^{H} \beta_r^s(z\gamma h - \sigma_{r0}) \cdot \ln\left(\frac{t_2}{t_1}\right) dh \tag{8}$$

Finally, solving the previous integration and rearranging yields

$$\frac{\Delta H}{H} \approx \beta_r^s \left[\frac{1}{2}\left(z\gamma H + \frac{\sigma_{r0}^2}{z\gamma H}\right) - \sigma_{r0}\right] \ln\left(\frac{t_2}{t_1}\right) \tag{9}$$

Eq. (9) yields an analytical closed-form solution for postconstruction crest settlement of a rockfill embankment before application of external loads.

In Eq. (9), assuming that β_r^s is constant, the crest settlement per dam height changes linearly with logarithm of time. The crest settlement patterns observed in the field, as presented in Fig. 7, are also almost linear in semilog scale. Therefore, the field settlement pattern is consistent with the analytical solution, as well as the aforementioned assumptions for the behavior of internal rockfill layers.

To obtain β_r^s for the rockfill used in each CFRD, Eq. (9) was rewritten in differential form

$$d\left(\frac{\Delta H}{H}\right) \Big/ d(\ln t) \approx \beta_r^s \left[\frac{1}{2}\left(z\gamma H + \frac{\sigma_{r0}^2}{z\gamma H}\right) - \sigma_{r0}\right] \tag{10}$$

The left side of Eq. (10) is the rate of crest settlement relative to dam height in natural logarithmic scale. Therefore, it is the same parameter as α_1 defined in Fig. 7 but with a different log base: $d(\Delta H/H)/d(\ln t) = \alpha_1/\ln 10$. Moreover, all of the parameters inside the brackets in the right-hand side of Eq. (10) were available. The values of γ and H are presented in Table 1; the reduction factors z were calculated by using simple numerical models, as noted previously; and, the σ_{r0} values were estimated according to the intact rock UCS, as explained in the previous section. Thus, the β_r^s values were back-calculated for each studied CFRD knowing all other parameters in Eq. (10).

β_r^s as a Function of Rockfill Index Properties

Fig. 10 shows the calculated β_r^s values versus the corresponding rockfill void ratio at placement for each CFRD. Similar to previous parts, the CFRD cases are categorized according to intact rock UCS. First, the calculated β_r^s values are in the same range as observed by Oldecop and Alonso (2007) and Romero et al. (2012) in laboratory oedometer tests.

Second, in Fig. 10, the parameter β_r^s is clearly higher for the cases with rockfill quarried from lower-strength rock. The β_r^s has an almost constant value for all of the rockfills quarried from very-high-strength rock, with a slight increase with increasing void ratio. This can be attributed to the small number of fissures and cracks in rock particles, so that an increase in stress level triggers only a few cracks to propagate with time. Thus, the effect of stress level on time-dependent compressibility does not clearly vary from one case to another. Similar to the trends observed for the rockfill moduli (Fig. 5), Bastyan Dam lies between the data points associated with the two strength categories.

In Fig. 10, for cases with medium to high intact rock strength, the parameter β_r^s increases with increasing rockfill void ratio. Higher void ratio leads to less contact points and thus to higher contact point stress and higher crack stress intensities (as explained in the mechanism of rockfill deformation). Consequently, rockfills placed at higher void ratio show clearer time-dependent response to increases in applied load. The β_r^s-void ratio point obtained for the rockfill of Winneke Dam falls between the data sets related to the two categories. The average UCS reported for this case is 66 MPa, which is very close to the boundary between high and very high intact strength categories. This might also be why the data point for Bastyan Dam falls between the two categories [Fig. 5(a)].

In summary, at the vertical stress range normally experienced in rockfill dams (less than 3 MPa), rockfill time-dependent compressibility in quasi-oedometric conditions (negligible lateral deformations) can be characterized with two parameters, σ_{r0} and β_r^s. The parameter σ_{r0} is a threshold stress that defines the onset of rockfill time-dependent deformations. The parameter β_r^s defines the slope of increases in time-dependent compressibility with increasing vertical stress level. Both parameters can be roughly estimated knowing rockfill void ratio and the average strength of intact parent rock. Given these two parameters, the postconstruction crest settlement can be estimated by using Eq. (9). This equation is valid for the period before application of external loads (e.g., reservoir and traffic) or when the external loads are negligible compared with the embankment self-weight. Estimation of the postconstruction settlements during reservoir filling and during the operation period based on constructional data is not included in this paper.

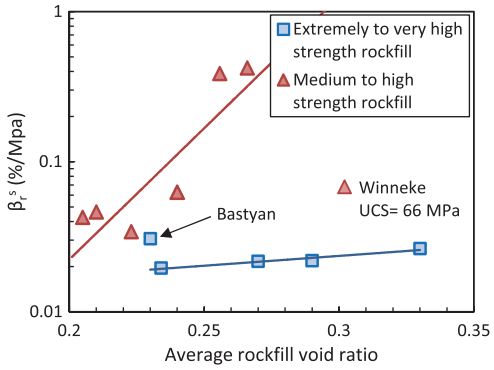

Fig. 10. Slope of changes in time-dependent compressibility index with vertical stress, β^s, versus the average rockfill void ratio at placement

Table 3. Parameters Obtained for the Rockfill Used in the Studied CFRDs

Dam name	σ_{ry} (kPa)	M_{ri} (MPa)	M_{rb} (MPa)	α_1	σ_{r0} (kPa)	β_r^s (%/MPa)
Reece	—	159.0	—	0.026	700	0.010
Bastyan	—	118.6	—	0.022	400	0.015
Cethana	880	259.1	114.4	0.027	400	0.013
Murchison	970	304.2	147.1	0.022	400	0.011
Foz Do Areia	700	51.0	36.8	0.059	400	0.019
Shuibuya	—	—	74.6	—	—	—
Winneke	—	—	—	0.064	200	0.068
Kotmale	800	88.8	37.4	0.059	200	0.043
White Spur	—	88.0	—	0.023	200	0.046
Tullabardine	—	64.6	—	—	—	—
Mackintosh	800	53.5	31.7	0.093	200	0.063
Little Para	—	—	—	0.035	0	0.034
Scotts Peak	—	—	—	0.360	0	0.422
Roadford	500	26.0	20.9	—	—	—
Martin Gonzalo	660	13.9	7.1	0.329	0	0.387

A summary of the calculated parameters for short-term and time-dependent compression of the studied cases is presented in Table 3.

Short-Term versus Time-Dependent Compressibility

Relationship between Short-Term and Time-Dependent Compressibility in Oedometer Tests

λ and λ^t (defined in Fig. 6) can be respectively related to the compression index C_c and secondary compression coefficient C_α calculated in consolidation tests on soils ($C_c = \Delta e/\Delta \log \sigma$ and $C_\alpha = \Delta e/\Delta \log t$). The only difference is that in defining λ^t and λ, one uses the axial strain instead of the void ratio, and natural logarithm instead of decimal logarithm. Thus, for a given series of oedometer test data, $C_\alpha/C_c = \lambda^t/\lambda$. Studies on various oedometer tests on earth materials show that C_α/C_c ratio is almost constant for a specific material at different stress levels. The studied earth materials included clay (Mesri and Godlewski 1977), sand (Mesri et al. 1990; Mesri and Vardhanabhuti 2009), and rockfill (Oldecop and Alonso 2007). This aspect will be further studied using the λ^t and λ values obtained from analysis of the real CFRDs instrumentation data.

Relationship between In-Situ Short-Term and Time-Dependent Compressibilities

Fig. 11 shows the back-calculated λ_r^t versus the λ_r values obtained from in situ vertical stress-strain curves at different vertical stress levels. The data points fell almost on straight lines, as it is generally observed for earth materials. The λ_r^t versus λ_r values are also well inside the range reported in the literature. Apart from the data points associated with Martin Gonzalo Dam, the ratio λ_r^t/λ_r varies between 0.0065 and 0.03. This ratio was observed to vary between 0.01 and 0.03 in oedometer tests on granular soils as mentioned by Mesri et al. (1990) and Mesri (2007) or between 0.004 and 0.025 based on suction-controlled one-dimensional compression tests on rockfill as reported by Alonso et al. (2013). This validates the presented analytical approach to find rockfill in situ time-dependent compressibility parameters. It is also interesting that the λ_r^t/λ_r range implied from field data is close to that already observed in the laboratory.

The construction period of a CFRD can take several years. Thus, some of the time-dependent deformations occur in the construction stage. Therefore, the calculated λ_r^t values might have been underestimated. Therefore, the λ^t/λ values could have been considerably larger in the field than in the laboratory, if the creep deformations during construction had been taken into account.

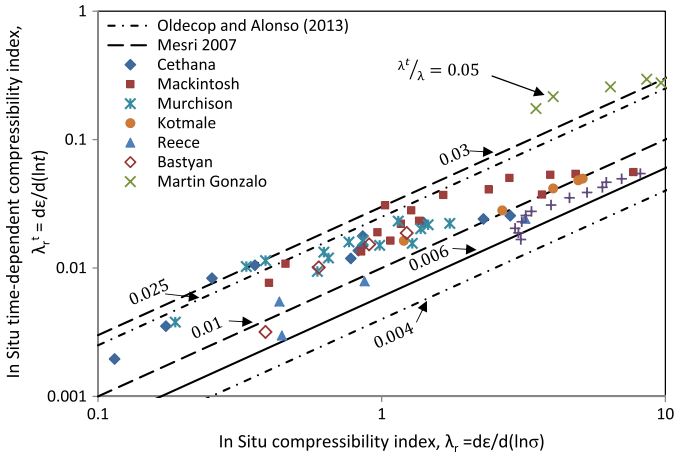

Fig. 11. Time-dependent compressibility index versus the compressibility index of rockfill obtained from the back-analysis of the studied CFRDs

The upper band in Fig. 11 belongs to Martin Gonzalo Dam, where excessive settlements caused by heavy precipitations and susceptibility of rockfill to wetting collapse were reported. This is in agreement with Oldecop and Alonso (2007), who reported higher λ^t/λ values for samples with higher relative humidity of the air passing through the sample compared with other samples.

In Fig. 11, for cases like Foz do Areia and Bastyan, λ_r^t values seem to have been underestimated at low stress levels. This could be attributed to the simplification adopted in λ_r^t versus vertical stress curves. At stresses less than σ_{r0}, λ_r^t was assumed to equal zero [Fig. 6(d)]. Such simplification seems to underestimate λ_r^t values for the stresses close to σ_{r0}. The trends observed in Fig. 11 also validate the assumption that, throughout typical CRFD applied stress ranges, λ_r^t increased with stress level; i.e., the internal vertical stresses did not exceed σ_c in Fig. 6(d). The reason is that, if σ_c was surpassed, at high stress levels, λ_r^t values would have been overestimated, and consequently, the λ_r^t/λ_r values would have increased beyond the general linear trend, which is not the case in this figure.

For the data of eight CFRDs presented in Fig. 11, a limited range was found for the in situ λ_r^t/λ_r values (primarily between 0.0065 and 0.03). This implies that, in general, when λ_r values were high for a given rockfill, λ_r^t were also high, and vice versa. In other words, when rockfill material was more compressible during construction, it continued to deform significantly during the postconstruction period. This suggests that knowing the behavior of rockfill layers during construction of a rockfill embankment, one can have an estimation of its postconstruction behavior. This approach can be used to find guidelines for predicting long-term settlements of rockfill embankments on the basis of their settlements during construction. Finding such guidelines is the subject of further research (Kermani et al. 2016).

Conclusions

In this study, the in situ mechanical behavior of rockfill during and after construction of 15 CFRDs was studied. It was shown that the rockfill vertical stress-strain relation obtained at quasi-oedometric

conditions in the field can be estimated with two straight lines. The slopes of these lines, M_{ri} and M_{rb}, were comparable with constrained moduli in laboratory oedometer tests on coarse granular materials. The stress at which the slope changes, σ_{ry}, could be related to change in deformation mechanism from sliding to breakage of particles. Moreover, a closed-form equation for the time-dependent crest settlement of a rockfill embankment under self-weight load was introduced. In this equation, two parameters were used to define rockfill time-dependent deformations: β_r^s, which defines the slope of increase in time-dependent compressibility index with increasing vertical stress; and σ_{r0}, which is a threshold stress for the onset of time-dependent deformations.

By evaluating the data on CFRD case studies, the in situ short-term compressibility parameters (M_{ri}, M_{rb}, and σ_{ry}) and the time-dependent compressibility parameters (σ_{r0} and β_r^s) were back-calculated. The obtained parameters were shown to depend on intact rock strength and rockfill void ratio at placement. In addition, the well-known concept that the C_α/C_c ratio is almost constant for a given earth material was evaluated and verified for the rockfill of the studied CFRDs. It was suggested that this concept could be used for predicting long-term settlements of rockfill structures on the basis of their index properties and mechanical behavior during construction.

Acknowledgments

The authors gratefully acknowledge the financial support of the Natural Sciences and Engineering Research Council of Canada (NSERC)—Hydro-Québec Industrial Research Chair for lifecycle optimization of embankment dams. The authors also extend their appreciation to their industrial partners: Hydro-Québec, SNC-Lavalin, Qualitas, WSP, Golder Associates, Klohn Crippen Berger, ConeTec, and Hatch. Finally, the authors thank the University of New South Wales for permission to publish the data related to the dams.

Supplemental Data

Figs. S1–S6 and a description of the limitations of the study are available online in the ASCE Library (www.ascelibrary.org).

References

Alonso, E. (2003). "Exploring the limits of unsaturated soil mechanics: The behavior of coarse granular soil and rockfill." *Proc., 11th Buchanan Lecture*, Univ. of Texas A&M, College Station, TX.

Alonso, E., Tapias, M., and Gili, J. (2013). "Particle crushing, scale effects and delayed behaviour of rockfill. A DEM investigation." *Proc., Alter Workshop Degradation in Geomaterials*, Aussois, France.

Alonso, E. E., Olivella, S., and Pinyol, N. M. (2005). "A review of Beliche Dam." *Géotechnique*, 55(4), 267–285.

Alonso, E. E., Olivella, S., Soriano, A., Pinyol, N. M., and Esteban, F. (2011). "Modelling the response of Lechago earth and rockfill dam." *Géotechnique*, 61(5), 387–407.

Alonso, E. E., Tapias, M., and Gili, J. (2012). "Scale effects in rockfill behaviour." *Géotech. Lett.*, 2(3–9), 155–160.

AS (Australia Standards). (1993). "Geotechnical site investigations." *AS 1726-1993*, Homebush, NSW, Australia.

Charles, J. A. (1973). "Correlation between laboratory behaviour of rockfill and field performance with particular reference to Scammonden Dam." Ph.D. thesis, London Univ., London.

Clements, R. P. (1981). "The deformation of rockfill; inter-particle behaviour, bulk properties and behaviour in dams." Ph.D. thesis, King's College, London.

Clements, R. P. (1984). "Post-construction deformation of rockfill dams." *J. Geotech. Eng.*, 10.1061/(ASCE)0733-9410(1984)110:7(821), 821–840.

Colliat-Dangus, J. L., Desrues, J., and Foray, P. (1988). "Triaxial testing of granular soil under elevated cell pressure." *ASTM STP 977*, ASTM, West Conshohocken, PA, 290–310.

Dascal, O. (1987). "Postconstruction deformations of rockfill dams." *J. Geotech. Eng.*, 10.1061/(ASCE)0733-9410(1987)113:1(46), 46–59.

Das Neves, E. M., and Veiga Pinto, A. (1988). "Modelling collapse on rockfill dams." *Comput. Geotech.*, 6(2), 131–153.

Evans, J. D., and Wilson, A. C. (1992). "The instrumentation, monitoring and performance of Roadford Dam during construction and first filling." *Proc., 7th Conf. of British Dam Society*, Thomas Telford, London, 157–165.

Evans, J. D., and Wilson, A. C. (1994). "The asphalt membranes at Colliford and Roadford Reservoirs J.D." *Proc., 8th Conf. of British Dam Society*, Thomas Telford, London, 1–11.

Fitzpatrick, M. D., Cole, B. A., Kinstler, F. L., and Knoop, B. (1985). "Design of concrete-faced rockfill dams." *Proc., Symp. on Concrete Face Rockfill Dams—Design, Construction and Performance*, ASCE, Reston, VA, 410–434.

Guiyao, W., Zongying, H., and Jianlin, J. (2009). "Construction technique for high CFRD." *Proc., 1st Int. Symp. on Rockfill Dams*, Chinese National Committee on Large Dams and Brazilian Committee on Large Dams, Chengdu, China.

Hunter, G., and Fell, R. (2002). "The deformation behaviour of rockfill." *Uniciv Rep. No. R-405*, Univ. of New South Wales, Sydney, Australia.

Hunter, G., and Fell, R. (2003). "Rockfill modulus and settlement of concrete face rockfill dams." *J. Geotech. Geoenviron. Eng.*, 10.1061/(ASCE)1090-0241(2003)129:10(909), 909–917.

Justo, J. L. (1991). "Collapse: Its importance, fundamentals and modelling." Chapter 6, *Advances in rockfill structures*, Springer, Dordrecht, Netherlands, 97–152.

Justo, J. L., Canete, P., Manzanares, J. L., Del Campo, J., and De Porcellinis, P. (1988). "The upstream facing of Martin Gonzalo rockfill dam." *Proc., 16th Int. Congress on Large Dams (ICOLD)*, International Commission on Large Dams, San Francisco, 815–837.

Justo, J. L., and Durand, P. (2000). "Settlement-time behaviour of granular embankments." *Int. J. Numer. Anal. Methods Geomech.*, 24(3), 281–303.

Kermani, M., Konrad, J., and Smith, M. (2016). "An empirical method for predicting post-construction settlement of concrete face rockfill dams." *Can. Geotech. J.*, 54(6), 755–767.

Kjaernsli, B., and Sande, A. (1963). "Compressibility of some coarse-grained materials." *Proc., 1st European Conf. on Soil Mechanics and Foundation Engineering*, Weisbaden, Germany, 245–251.

Konrad, J. M., and Boisvert, L. (2010). "Essais de compression oedométrique sur matériau de remblai en enrochement: Granulométries médiane et uniforme." *Rapport GCT-2010-04-03*, Université Laval, Québec (in French).

Marachi, N. D., Chan, C. K., Seed, H. B., and Duncan, J. M. (1969). "Strength and deformation characteristics of rockfill materials." *Rep. No. TE*, Univ. of California, Berkeley, CA.

Marsal, R. J. (1967). "Large-scale testing of rockfill materials." *J. Soil Mech. Found. Div.*, 93(2), 27–43.

Marsal, R. J. (1973). "Mechanical properties of rockfill." *Embankment dam engineering—Casagrande volume*, R. C. Hirschfeld and S. J. Poulos, eds., Wiley, New York, 109–200.

McDowell, G. R., and Bolton, M. D. (1998). "On the micromechanics of crushable aggregates." *Géotechnique*, 48(5), 667–679.

Mesri, G. (2007). "Discussion: Theoretical investigation of the time-dependent behaviour of rockfill." *Géotechnique*, 57(9), 779–781.

Mesri, G., Feng, T. W., and Benak, J. M. (1990). "Postdensification penetration resistance of clean sands." *J. Geotech. Eng.*, 10.1061/(ASCE)0733-9410(1990)116:7(1095), 1095–1115.

Mesri, G., and Godlewski, P. M. (1977). "Time- and stress-compressibility interrelationship." *J. Geotech. Eng. Div.*, 103(GT5), 417–430.

Mesri, G., and Vardhanabhuti, B. (2009). "Compression of granular materials." *Can. Geotech. J.*, 46(4), 369–392.

Milligan, V., and Coyne, L. (2005). "Review of factors influencing the settlement of rockfill dams." *Proc., K.Y. Lo Symp.*, Univ. of Western Ontario, London, 1–31.

Nobari, E. S., and Duncan, J. M. (1972). "Effect of reservoir filling on stresses and movements in earth and rockfill dams." *Rep. No. TE-72-1*, Univ. of California, Berkeley, CA.

Oldecop, L. A., and Alonso, E. E. (2001). "A model for rockfill compressibility." *Géotechnique*, 51(2), 127–139.

Oldecop, L. A., and Alonso, E. E. (2007). "Theoretical investigation of the time-dependent behaviour of rockfill." *Géotechnique*, 57(3), 289–301.

Ortega, E. F. (2008). "Comportamiento de materiales granulares gruesos. Efecto de la succión." Ph.D. thesis, Universitat Politècnica De Catalunya, Barcelona, Spain (in Spanish).

Parkin, A. K. (1991). "Creep of rockfill." *Advances in rockfill structures*, E. M. das Neves, ed., Kluwer Academic Publishers, Dordrecht, Netherlands, 221–237.

Pestana, J. M., and Whittle, A. (1995). "Compression model for cohesionless soils." *Geotechnique*, 45(4), 611–631.

Pinto, N. D. S., and Marques Filho, P. L. (1998). "Estimating the maximum face deflection in CFRDs." *Int. J. Hydropower Dams*, 5, 28–32.

Poulos, H. G., and Davis, E. A. (1974). *Elastic solutions for soil and rock mechanics*, Wiley, New York.

Romero, E., Alonso, E. E., Alvarado, C., and Wacker, F. (2012). "Effect of loading history on time dependent deformation of rockfill." *Unsaturated soils: Research and applications*, Springer, Berlin, 419–424.

Sowers, G. F., Williams, R. C., and Wallace, T. S. (1965). "Compressibility of broken rock and the settlement of rockfills." *Proc., 6th ICSMFE*, Vol. 2, University of Toronto Press, Montréal, 561–565.

Tavares, L. M., and das Neves, P. B. (2008). "Microstructure of quarry rocks and relationships to particle breakage and crushing." *Int. J. Miner. Process.*, 87(1), 28–41.

Wilson, A. C., and Evans, J. D. (1991). "The use of low grade rockfill at Roadford Dam." *The embankment dam*, Thomas Telford, London, 21–27.

Won, M.-S., and Kim, Y.-S. (2008). "A case study on the post-construction deformation of concrete face rockfill dams." *Can. Geotech. J.*, 45(6), 845–852.

Zhou, W., Hua, J., Chang, X., and Zhou, C. (2011). "Settlement analysis of the Shuibuya concrete-face rockfill dam." *Comput. Geotech.*, 38(2), 269–280.